Journal of the Meteorological Society of Japan, Vol. 88, No. 1, pp. 15–28, 2010.
DOI:10.2151/jmsj.2010-102

Linkage of the Boreal Spring Antarctic Oscillation to the West African Summer Monsoon

Jianqi SUN and Huijun WANG

Nansen-Zhu International Research Centre (NZC), Institute of Atmospheric Physics, Chinese Academy of Sciences, Beijing, China

Wei YUAN

China Meteorological Administration Training Centre, Beijing, China

(Manuscript received 5 July 2007, in final form 20 September 2009)

Abstract

The relationship between the boreal spring (or the austral autumn) Antarctic Oscillation (AAO) (March–April) and the West African summer monsoon (WASM) (June–September) is analyzed based on NCEP/NCAR reanalysis data. The results show that the linkage of the boreal spring AAO to the WASM exhibits decadal-scale variations: a strong connection between the two appears over the period 1985–2006 and a weak connection over the period 1970–1984. Further analysis indicates that such an unstable relationship between the two results from the modulation by ENSO events to a large extent.

A possible mechanism for the impacts of the boreal spring AAO on the WASM is also discussed. The variability of the boreal spring tropical South Atlantic sea surface temperature (SST) appears to serve as a bridge linking these two systems. The boreal spring AAO produces an anomalous SST over the tropical South Atlantic by exciting an equatorward Rossby wave train over the western Southern Hemisphere (SH). This AAO-related SST anomaly modulates the meridional gradient of moist static energy (MSE) between the Sahel and the Guinea-tropical Atlantic region in the boreal spring. The MSE gradient is of paramount importance for the changes from spring to summer in the West African monsoon because its relaxation along the seasonal cycle is linked to the northward excursion of the WASM system into the African continent. Therefore, an anomalous AAO-related MSE gradient can lead to anomalous Sahel rainfall in the early summer. When this rainfall occurs over the Sahel, the local positive soil moisture-rainfall feedback plays a crucial role in sustaining and prolonging this rainfall anomaly throughout the whole summer.

1. Introduction

The annual rainfall over the Sahel is characterized by a sharp meridional gradient, varying from 1200–1600 mm at the southern edge to 50–100 mm at the northern edge. The year-to-year standard deviation ranges from 10–20% of the annual mean at the southern edge to 50% at the northern edge (Nicholson 1980). The variability of the position and intensity of rain-belt over the Sahel is dominated by the West African summer monsoon (WASM) and is very important for the region's rain-fed agriculture, water resources, health, and climatically sensitive natural environments. The socio-economic and environmental shocks resulting from the dramatic decline in rainfall since the mid-1960s have produced widespread human misery and environmental degradation (Lister and Palutikof 2001).

Many studies have sought to understand the causes of the persistent droughts from the mid-1960s to the mid-1990s. These studies can be divided into two main groups. The first focused on

Corresponding author: Jianqi Sun, NZC, Institute of Atmospheric Physics, Chinese Academy of Sciences, P.O. Box 9804, Beijing 100029, China.
E-mail: sunjq@mail.iap.ac.cn

the role of local land forcing (e.g., changes of land cover). Charney's pioneering work (1975) on the land-atmosphere interaction in West Africa presented the well-known "Charney's hypothesis," which describes the positive feedback process between changes in the albedo and the Sahel's rainfall. Since then, many observational and modeling studies have been conducted (Charney et al. 1977; Sud and Molod 1988; Xue and Shukla 1993; Zheng and Eltahir 1998; Zeng et al. 1999; Wang and Eltahir 2000; Clark et al. 2001). These studies concluded that changes in local land surface conditions play an important role in the WASM variability. However, the extent to which the land-atmosphere feedback mechanism contributes to the African monsoon variability has not been clarified (Giannini et al. 2003).

The other group of studies emphasized the role of the ocean. They have shown that the WASM interannual variability can often be linked to sea surface temperature (SST) anomaly patterns. These involve changes in the tropical Atlantic (Hastenrath 1990; Lamb and Peppler 1992; Vizy and Cook 2001), the central and eastern Pacific (Rowell 2001; Janicot et al. 2001), the Indian Ocean (Shinoda and Kawamura 1994; Bader and Latif 2003), the Mediterranean Sea (Rowell 2003), and even more generally in the global oceans (Folland et al. 1986). For example, negative (positive) rainfall anomalies over the Sahel are associated with negative (positive) SST anomalies over the tropical North Atlantic and with positive (negative) SST anomalies over the tropical South Atlantic, the tropical eastern Pacific, and much of the Indian Ocean. These SST anomalies may lead to large-scale atmospheric circulation and rainfall changes over the Sahel by influencing moisture advection from the ocean to the monsoon region, affecting the deep convection region, and inducing an anomalous equatorial wave response (e.g., Rowell et al. 1995).

Thus, the tropical SST anomaly is recognized as a forcing mechanism for the Sahel rainfall. Some works have started to explore the possibility of using SST to predict Sahel rainfall using atmospheric general circulation models (Giannini et al. 2003; Bader and Latif 2003; Moron 2005). They have reproduced the spatial-temporal characteristics of the instrumental Sahel summer rainfall using only the observed SST as a forcing. However, various sources of errors decrease the potential predictability and skill of rainfall simulation. Moron (2005) argued that the percentage of SST-forced variance in seasonal rainfall levels over the Sahel is typically below 25–50% of their total variance. Thus, the sources of large portions of the variability of the Sahel rainfall remain unclear. Atmospheric variability and teleconnections may play important roles in the variability of the Sahel's rainfall and should be considered. For example, Rao and Sikka (2007) recently found that the Indian summer monsoon is closely related to the WASM on an intraseasonal time scale.

More recently, the Antarctic Oscillation (AAO) has been found to be related to the climate of the Northern Hemisphere, particularly to the East Asian summer monsoon (Xue et al. 2003; Gao et al. 2003; Wang and Fan 2005; Sun et al. 2009) and to dust event frequency through atmospheric teleconnections (Fan and Wang 2004). These linkages suggest that this remote southern atmospheric oscillation may also significantly affect climate variability in the Northern Hemisphere. The aim of this study is to investigate whether the AAO is also associated with the WASM.

This paper is divided into six sections. Section 2 introduces the data utilized in this study. Section 3 describes the relationship between the boreal spring AAO and the WASM. Section 4 explores a possible mechanism for the coupling of the boreal spring AAO and the WASM, while Section 5 discusses why the relationship between the two is unstable. Our findings are summarized in Section 6.

2. Datasets

The monthly atmospheric reanalysis dataset used in this study comes from the National Centers for Environmental Prediction/National Center for Atmospheric Research (NCEP/NCAR) global atmospheric reanalysis data (Kalnay et al. 1996). The variables include horizontal winds, geopotential height, specific humidity, and soil moisture, while the soil moisture is the model output. Outgoing long wave radiation (OLR) data, used to infer tropical convection, are provided by the NOAA/OAR/ESRL PSD, Boulder, Colorado, USA and is available from June 1974 onward with a missing period between March and December in 1978. In evaluating the NCEP/NCAR reanalysis data, Sterl (2004) pointed out that the data are strongly inhomogeneous and of very poor quality prior to the end of the 1960s in large parts of the SH, especially over the ocean, where the observations are short. Kidson (1999) and Hines et al. (2000) showed that the NCEP/NCAR reanalysis data from 1970

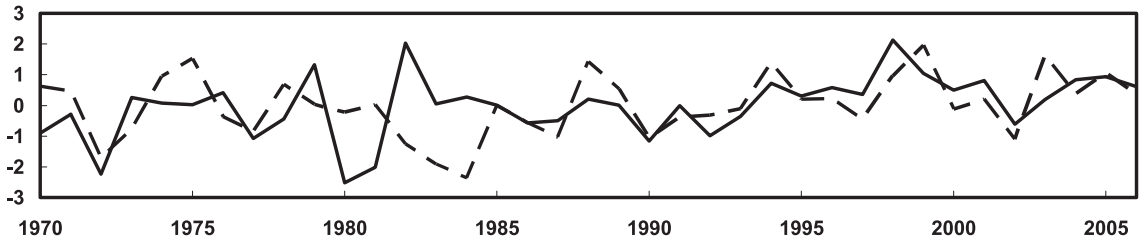

Fig. 1. Normalized time series of the boreal spring (March–April) AAO index (solid line) and the Sahel summer (June–September) rainfall index (dashed line).

onward could be acceptable for studies of climate variability in the southern high latitudes. Thus, in this study we will focus on the period 1970–2006.

The monthly SST dataset is from the version 2 of the NOAA Optimum Interpolation (OI) SST data (Reynolds et al. 2002), which is at a resolution of $1^\circ \times 1^\circ$ latitude/longitude and is available from November 1981 to the present.

Monthly mean rainfall data on a $2.5^\circ \times 2.5^\circ$ latitude/longitude grid are obtained from the Climate Prediction Center (CPC) Merged Analysis of Precipitation (CMAP), available from 1979 to the present (Xie and Arkin 1997).

The AAO index is defined by the leading principal component of sea level pressure (SLP) anomalies south of 20°S. A positive (negative) AAO index is characterized by negative (positive) SLP anomalies centered over the Antarctic and positive (negative) anomalies around 40°S–50°S (Gong and Wang 1999; Thompson and Wallace 2000). The Sahel rainfall index from Mitchell (http://jisao.washington.edu/) is the standardized average of the standardized rainfall records of 14 stations within 8°N–20°N, 20°W–10°E. The averaging region is based on the rotated principal component analysis of average June through September African rainfall in Janowiak (1988). Records for these 14 stations were obtained from the National Center for Atmospheric Research World Monthly Surface Station Climatology (WMSSC), which offers data from 1898–2006. These particular stations were chosen since they had complete or almost complete records for 1950–1993. The rainy season in the Sahel occurs from June to September, delivering approximately 90% of the total annual rainfall (Bader and Latif 2003; Lebel et al. 2003). Thus, in this study, the Sahel summer rainfall index refers to the average of the Sahel rainfall series from June through September.

3. Relationships between the boreal spring AAO and the WASM

Figure 1 shows the normalized time series of the AAO index in March–April and the Sahel summer (June–September) rainfall index for the period 1970–2006. The correlation between these two indices is low, with a coefficient of 0.32, indicating that over the whole period, the connection between the boreal spring AAO and WASM is weak. However, a more detailed investigation indicates that the relationship between the Sahel summer rainfall and the boreal spring AAO varies with time. After 1985, the boreal spring AAO and the Sahel summer rainfall varies in phase, with a correlation coefficient of 0.67 in 1985–2006 that is significant at the 95% confidence level (Table 1). Over the period of 1970–1984, in contrast, the variabilities of these two indices are highly inconsistent with one another, and their correlation coefficient is near zero (0.08). From Fig. 2, we note that correlations between the boreal spring AAO and the Sahel summer rainfall have become more positive with time, and that significant correlations only exist for the period after 1985.

In agreement with the above correlation analysis,

Table 1. Correlation coefficients between the Sahel summer rainfall index and the boreal spring AAO index as well as the ENSO indices (ENSO1 is the first principal component of the tropical Pacific basin SST and ENSO2 indicates the Southern Oscillation index), over the periods of 1970–1984 and 1985–2006. Bold characters denote that the correlation is significant at the 95% confidence level.

		ENSO-WASM	
Period	AAO-WASM	ENSO1	ENSO2
1970–1984	0.08	**−0.67**	**0.64**
1985–2006	**0.67**	−0.34	0.30

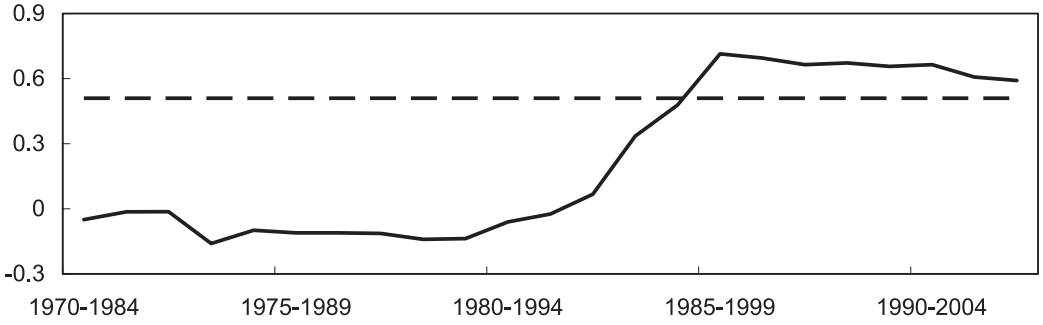

Fig. 2. Running correlations between the Sahel summer rainfall index and the AAO index with a 15-year window width for the period of 1970–2006. Dashed line indicates the 95% significance level.

the AAO-related atmospheric general circulations also differ in the WASM region for the period 1985–2006 and the period 1970–1984. Figure 3 displays regression maps of 200 hPa winds, 200 hPa divergence, 850 hPa winds, and OLR in July–September based on the boreal spring AAO index. At 200 hPa, there are significant easterly anomalies over the tropical Atlantic in the boreal summer corresponding to a positive-phase boreal spring AAO (Fig. 3a), which implies that the "Tropical Easterly Jet" (TEJ), an important component of the WASM (e.g., Grist and Nicholson 2001; Matthews 2004), is strengthened. In general, a strong TEJ can provide an upper-level divergence necessary for the development of convection that favors more rainfall over the Sahel (Figs. 3b,d). At 850 hPa, there are significant westerly anomalies over the West Africa-tropical Atlantic region in the boreal summer, the presence of which characterizes an enhanced WASM flow (Fig. 3c). The strengthened WASM flow blows inland from the ocean carrying more moisture and therefore also favors more rainfall over the Sahel (Fig. 3d). Thus, the boreal spring AAO is closely associated with WASM-related circulations during the period 1985–2006.

However, over the period 1970–1984, there are no significant atmospheric general circulation anomalies over the region of West Africa-tropical Atlantic in the boreal summer (Fig. 4), indicating that the connection between the boreal spring AAO and the WASM is broken in this period.

4. Possible mechanism for the connection between the boreal spring AAO and the WASM

4.1 How does the AAO affect the climate in the boreal spring?

How can the AAO, occurring in the middle to high latitudes of the SH, be linked to the WASM? Here, we will investigate whether some boreal spring climate systems may serve as a bridge between the AAO and the WASM, starting with an analysis of the tropical variation associated with the AAO over the period 1985–2006. The AAO and Sahel summer rainfall indices have a strong linear trend over the period 1985–2006 as depicted in Fig. 1. In particular, the linear trend of the AAO index is significant above the 95% confidence level. The linear trends for any time series are therefore removed in advance to highlight the interannual variability.

Figure 5 displays regression maps of March–April 200 hPa winds, 500 hPa geopotential height, and 850 hPa winds based on the boreal spring AAO index. It illustrates that, starting with the initial March–April period, the regression patterns at all levels exhibit a teleconnection wave train structure over the SH western hemisphere. A similar teleconnection pattern has been documented by Liebmann et al. (1999) and Cazes-Boezio et al. (2003). They concluded that this teleconnection pattern is likely to result from downstream dispersion of barotropic Rossby waves from the mid-latitude South Pacific. This possibility is well-reflected in the analysis of the AAO-related stationary wave activity. As the wave activity flux is parallel to the group velocity of stationary waves, it is a good indicator for the propagation of stationary waves in the atmosphere. Therefore a wave activity flux (W), formulated by Takaya and Nakamura (2001), is used to represent the horizontal propagation of quasi-stationary Rossby waves in the zonally inhomogeneous westerly. Setting the background meridional velocity to be zero, we can evaluate Plumb's (1985) flux. Its expression may be given as

$$\mathbf{W} = \frac{p}{2|\mathbf{U}|}\begin{bmatrix} U(\psi'_x - \psi'\psi_{xx}) + V(\psi'_x\psi'_y - \psi'\psi'_{xy}) \\ U(\psi'_x\psi'_y - \psi'\psi'_{xy}) + V(\psi'^2_y - \psi'\psi'_{yy}) \end{bmatrix},$$

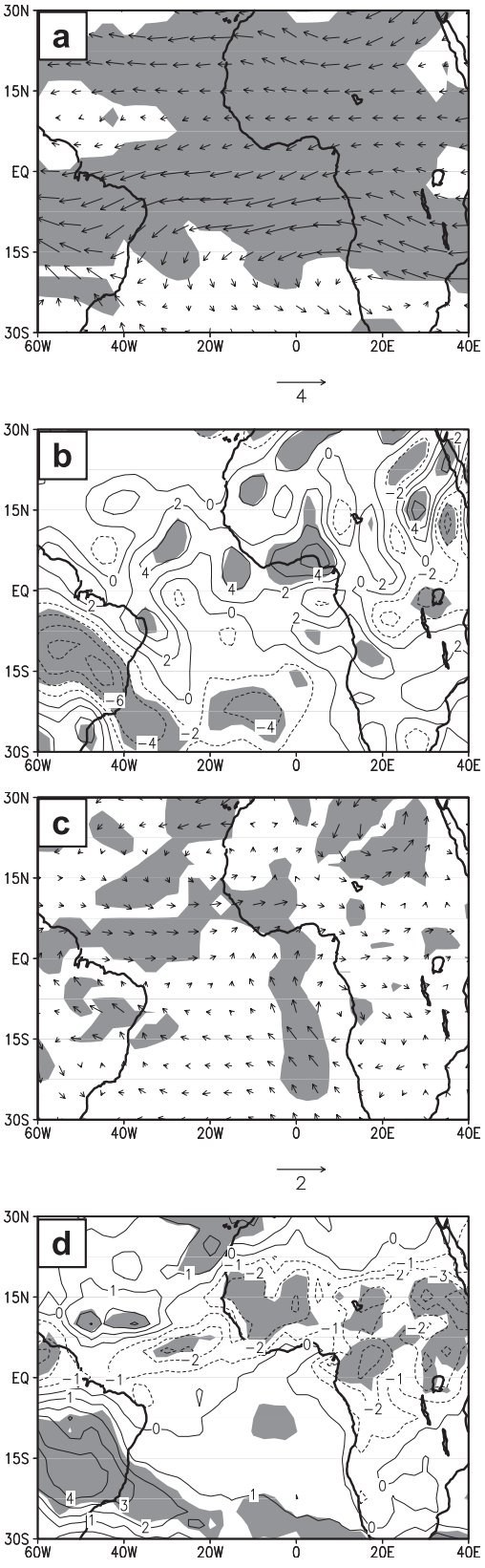

Fig. 3. Regression maps of (a) 200 hPa wind anomalies (m/s), (b) 200 hPa divergent anomalies (1/s), (c) 850 hPa wind anomalies (m/s), and (d) OLR anomalies (W/m^2) in July–September based on the boreal spring AAO index over the period 1985–2006. Shading indicates 95% statistical significance.

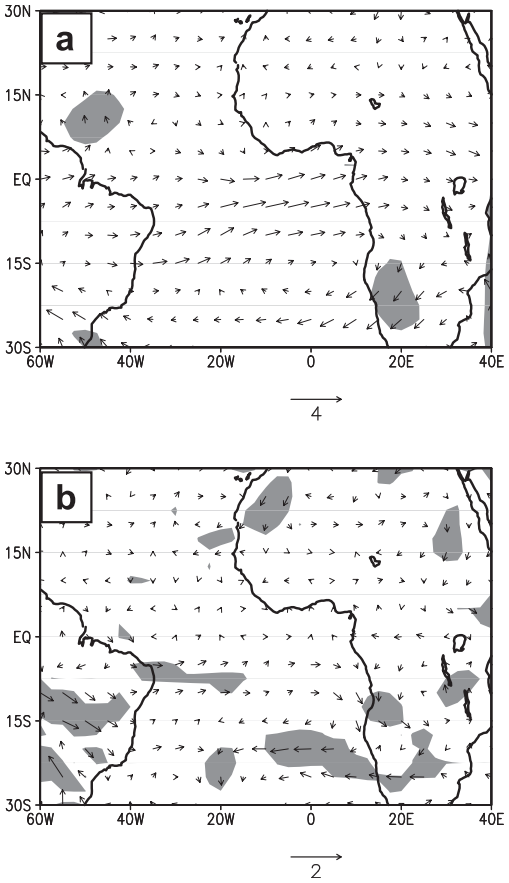

Fig. 4. Regression maps of (a) 200 hPa and (b) 850 hPa wind anomalies (m/s) in July–September based on the boreal spring AAO index over the period 1970–1984. Shading as in Fig. 3.

where ψ' denotes stream function anomalies regressed upon the AAO index, subscripts partial derivatives, $\mathbf{U} = |U, V|$ the basic-flow velocity, and p the normalized pressure (pressure/1000 hPa). Here, the mean field over the period 1985–2006 is regarded as the basic state. As shown in Fig. 6, in an anomalous AAO boreal spring there is eastward

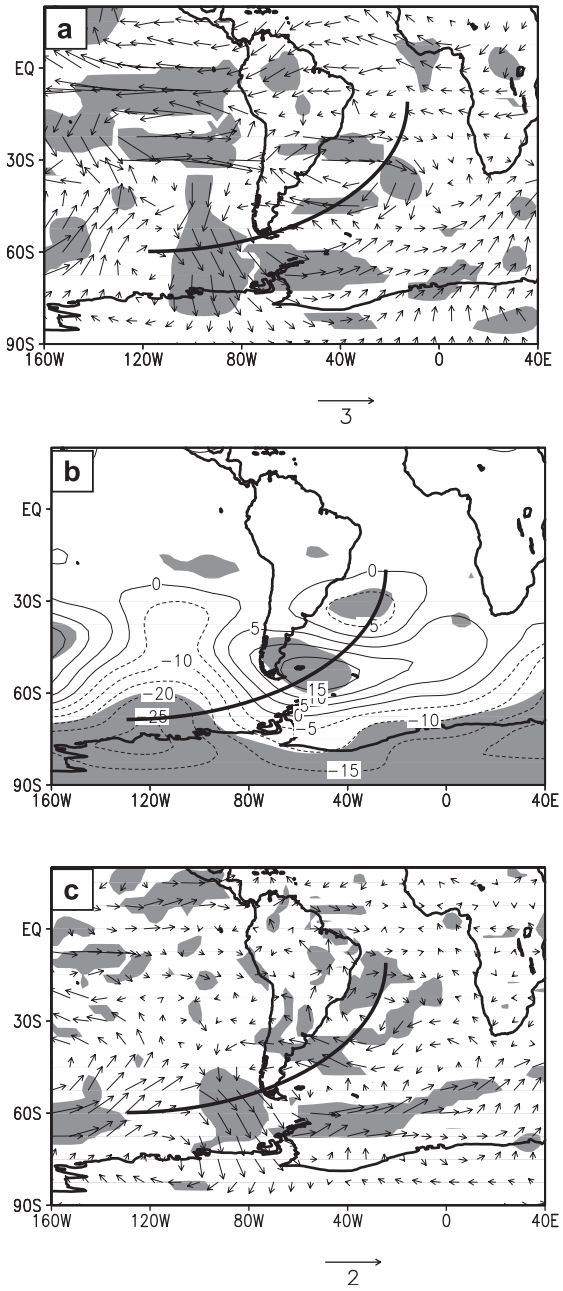

Fig. 5. Regression maps of (a) March–April 200 hPa wind anomalies (m/s), (b) 500 hPa geopotential height anomalies (gpm), and (c) 850 hPa wind anomalies (m/s) based on the boreal spring AAO index over the period 1985–2006. Shading as in Fig. 3.

wave propagation over the middle-to-high SH latitudes. In addition, along the teleconnection path in Fig. 5, there is also equatorward wave propagation from the mid-latitude South Pacific.

Figure 7 shows a similar regression pattern to that in Fig. 6 but for May–June. This similarity suggests that the teleconnection pattern persists and intensifies. In general, the atmosphere does not have a long-term memory because of the chaotic nature of atmospheric motion. However, it should be noted that the atmospheric teleconnection pattern is accompanied by underlying SST teleconnection anomalies (Fig. 8). Such a persistent atmospheric teleconnection pattern in the boreal spring is likely to be maintained by local atmosphere-ocean interactions. Previous observational and modeling works have indicated that extratropical SST anomalies are primarily controlled by the overlying atmospheric conditions, such as wind stress, temperature, and humidity (e.g., Frankignoul and Reynolds 1983; Luksch and von Storch 1992; Miller et al. 1994). With a high AAO index, Antarctic cooling is due to the increased isolation of Antarctica by enhanced westerlies (Thompson and Solomon 2002). The warming in the Antarctic Peninsula region results from the strengthened northwesterly anomalies there, which bring relatively warm seawater and air. The cooling of the region (40°–60°S, 160°–120°W) is closely related to the southwesterly anomalies at the rear of the anomalous depression over the high-latitude South Pacific, which bring cold seawater and air from the Ross Sea. To the southeast of Brazil, cooling is mainly caused by the advection of relatively cold seawater and air from the high-latitude South Atlantic, due to the southerly anomalies between the anomalous anticyclone at the Antarctic Peninsula and anomalous depression at the South Atlantic. The westerly anomalies in the tropical South Atlantic weaken the easterly trade winds, in turn reducing the surface latent heat loss, favoring warming of the tropical South Atlantic. On the other hand, the SST anomalies would positively feed back to the overlying atmospheric system by exchanging heat fluxes between atmosphere and ocean, consequently enhancing the variability and persistence of the overlying atmospheric circulation regimes (Deser and Timlin 1997; Kushnir et al. 2002). Thus, although the March–April AAO anomaly vanishes by May–June, the related teleconnection pattern is still persistent. Similar positive atmosphere-ocean interactions in the extratropics have also been ob-

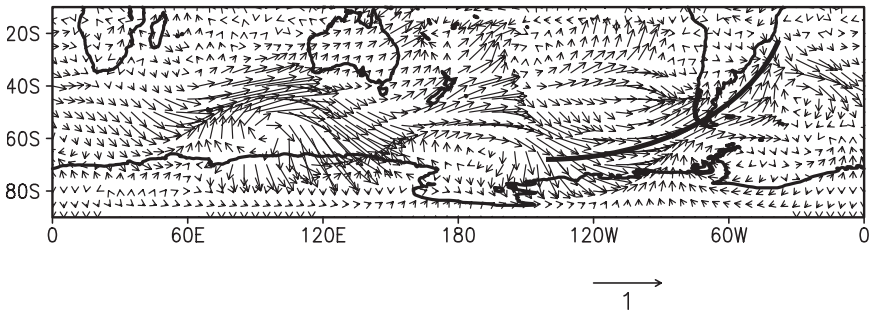

Fig. 6. The 500 hPa horizontal stationary wave activity flux (m^2/s^2) in March–April associated with the boreal spring AAO pattern for total wave numbers.

served and modeled by other studies (e.g., Palmer and Sun 1985; Wallace et al. 1990; Ferranti et al. 1994; Deser and Timlin 1997; Wang et al. 2001; Kushnir et al. 2002).

4.2 Roles of the anomalous SST over the tropical south atlantic

Figure 8 indicates that the AAO can induce an anomalous SST in the tropical South Atlantic through the aforementioned teleconnection pattern in the boreal spring. Some previous studies noted that the boreal spring's anomalous SST over the tropical South Atlantic has a delayed impact on the following summer's Sahel rainfall, with a warm SST corresponding to a wetter Sahel summer (e.g., Zheng et al. 1999). We confirm this correlation (Fig. 9). The WASM-related boreal spring tropical Atlantic SST anomalies are quite similar to the boreal spring AAO-related SST anomalies over the region. Thus the SST over the tropical South Atlantic in the boreal spring may serve as a bridge linking the boreal spring AAO and Sahel summer rainfall.

Eltahir and Gong (1996) pointed out the important role of boundary layer entropy in the dynamics of West African monsoon. Moreover, Zheng et al. (1999) and Fontaine et al. (2002) revealed the influence of the spring moist static energy (MSE) meridional gradient on the WASM spring to summer transition. They pointed out that before the wettest (driest) Sahel rainy seasons the MSE meridional gradients tend to be stronger (weaker) and tend to relax later (earlier) in the boreal spring. In this study, the AAO-related warm SST over the tropical South Atlantic can enhance its overlying boundary layer MSE (Fig. 10). The enhanced MSE in turn strengthens the meridional MSE gradient between the Guinea-tropical South Atlantic region and the Sahel. When the strong MSE meridional gradient relaxes along the seasonal cycle from the boreal spring to summer, it results in a strong WASM (Fontaine et al. 2002). Thus, the boreal spring AAO can affect the WASM through its impact on the boreal spring tropical South Atlantic SST and MSE meridional gradient over the regions of the Sahel and Guinea. When summer rainfall occurs over the Sahel, the local positive soil moisture-rainfall feedback (Fig. 11) plays a crucial role in sustaining and prolonging the anomalous summer rainfall (e.g., Zheng et al. 1999). The positive feedback process is simplified by Zheng et al. (1999), who point out that, on one hand, rainfall can moisten the soil of the region, while on the other hand, moistened soil results in lowered surface albedo and larger surface evaporation, which further enhance net surface radiation. The enhanced net surface radiation then increases the boundary layer entropy. The increased boundary layer entropy tends to destabilize the atmosphere and favor more rainfall at local scale, and also strengthen the monsoon circulation by enhancing the gradient of the boundary layer entropy on a large scale. Thus, the rainfall anomaly can persist in the boreal summer even after the disappearance of the boreal spring SST anomaly in the tropical Atlantic (Fig. 12).

5. Discussion of the weak relationship between the boreal spring AAO and WASM for the period from 1970 to 1984

The analysis in Section 3 shows that the relationship between the boreal spring AAO and WASM varies with time, a characteristic which parallels the unstable relationship between the El Niño/Southern Oscillation (ENSO) and the WASM (Janicot et al. 2001). More interesting, the weak linkage

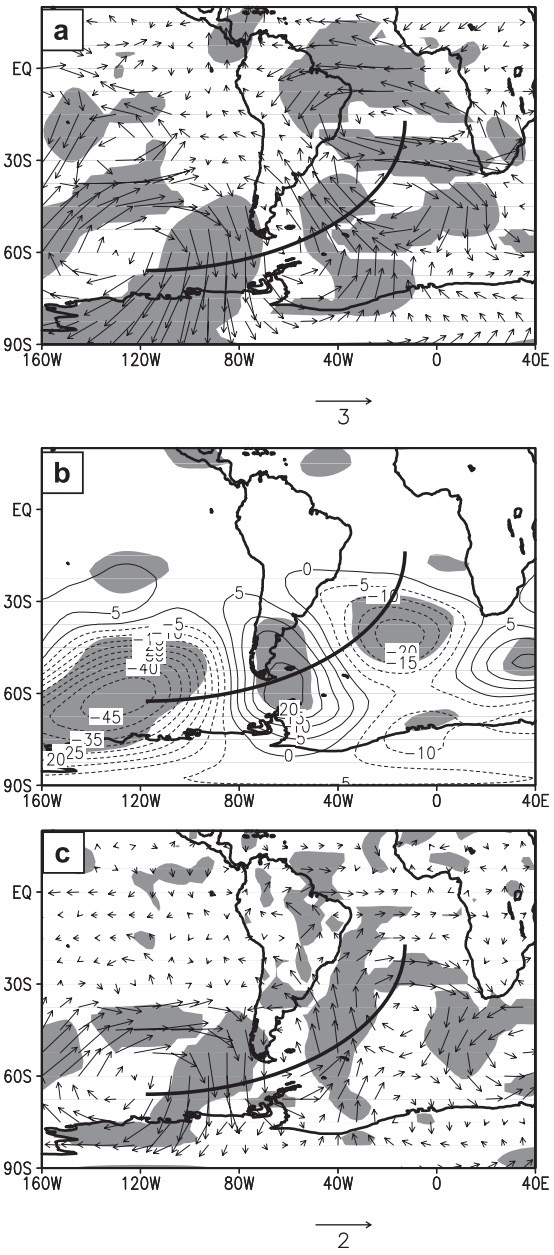

Fig. 7. Regression maps of (a) May–June 200 hPa wind anomalies (m/s), (b) 500 hPa geopotential height anomalies (gpm), and (c) 850 hPa wind anomalies (m/s) based on the boreal spring AAO index over the period 1985–2006. Shading as in Fig. 3.

between the boreal spring AAO and WASM appears over a period (1970–1984) when the correlation between ENSO and the WASM is strong (Table 1). Hence, the weak connection between the

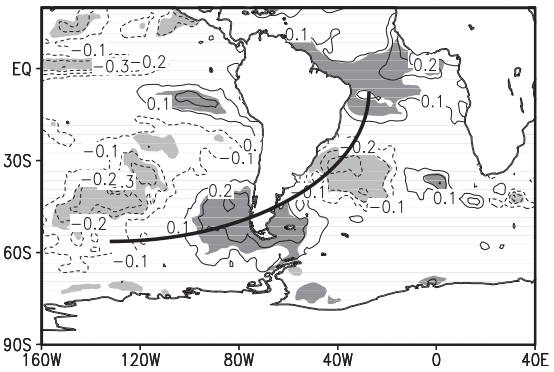

Fig. 8. Regression map of March–June SST anomalies (°C) based on the boreal spring AAO index over the period 1985–2006. Shading as in Fig. 3.

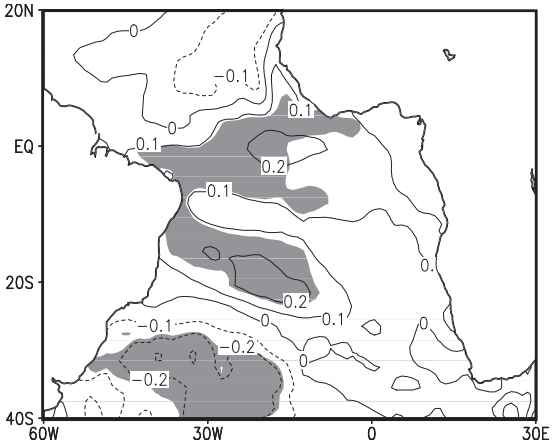

Fig. 9. Regression map of March–June SST anomalies (°C) based on the Sahel summer rainfall index over the period 1985–2006. Shading as in Fig. 3.

boreal spring AAO and WASM might result from modulation by ENSO events.

Figure 13 shows the correlations between the 850 hPa zonal wind and the ENSO1 index (the ENSO1 index is defined as the first principal component of the tropical Pacific basin SST) in the boreal spring and summer during the period of 1970–1984. As shown in the figure, there is a strong anomalous zonal wind in an anomalous ENSO year, implying that a strong ENSO signal dominates the tropics and is the main contribution to tropical climate and atmosphere variability when ENSO happens over this period. We next calculate the correlation between the ENSO1 index and the

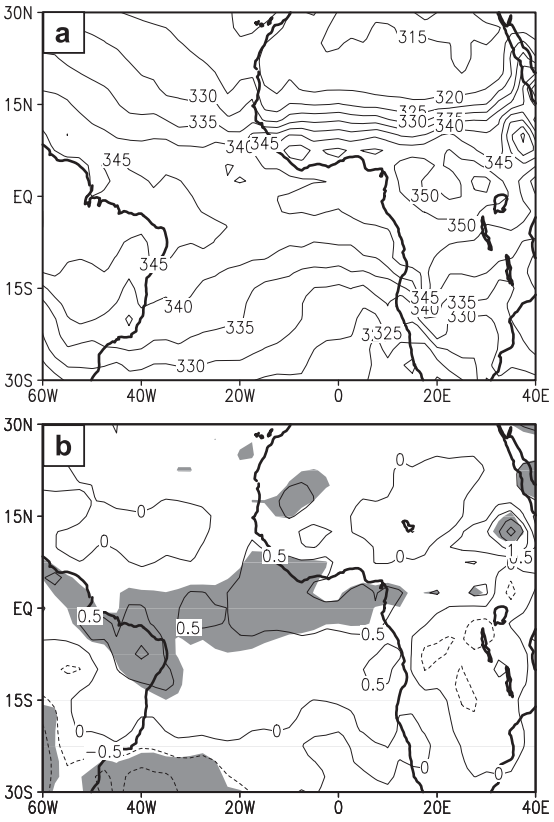

Fig. 10. (a) Climatology of the 1000 hPa MSE (KJ/Kg) in March–June and (b) regression map of March–June 1000 hPa MSE anomalies (KJ/Kg) based on the boreal spring AAO index over the period 1985–2006. Shading as in Fig. 3.

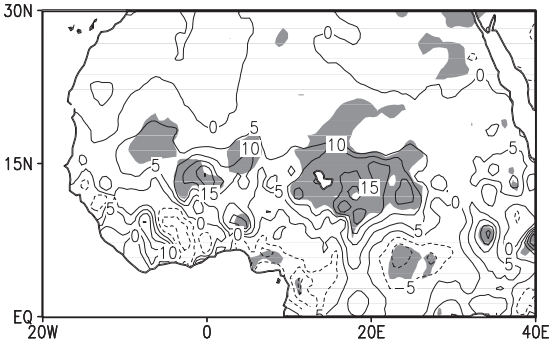

Fig. 11. Regression map of June–September soil moisture anomalies (mm) based on the Sahel summer rainfall index over the period 1985–2006. Shading as in Fig. 3.

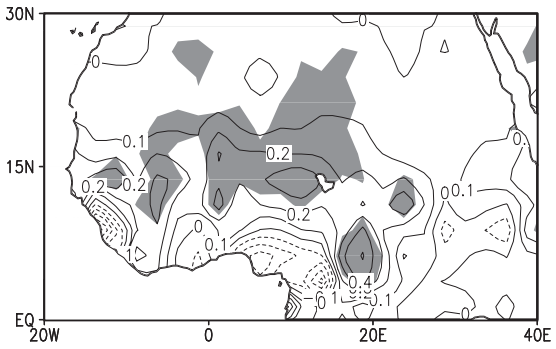

Fig. 12. Regression map of June–September CMAP precipitation anomalies (mm/day) based on the boreal spring AAO index over the period 1985–2006. Shading as in Fig. 3.

tropical Atlantic zonal wind index, which is defined as the mean 850 hPa zonal wind over the region (40°W–10°E, 10°S–5°N) in the boreal spring. The correlation is −0.88, which means that more than 77% of the total variance of the tropical Atlantic circulation can be attributed to the ENSO event (the explained variance equals the square of the correlation (Huang 2004)). In this period, the maximum variance attributable to other factors is less than 23%. We suppose an extreme situation, namely that this 23% variance is entirely attributed to the AAO variability. In this case, the maximum of the correlation coefficients between the AAO and tropical Atlantic zonal wind indices is less than 0.48, which is not significant at the 95% confidence level. In addition, in the period of 1970–1984, an anomalous AAO year always corresponds to an ENSO year as shown in Fig. 14, and the amplitude of the AAO anomaly is generally smaller than that of the ENSO event. Thus, in the presence of a strong ENSO event, the AAO could not produce significant circulation and SST changes over the tropical Atlantic. Consequently, the connection between the AAO and Sahel summer rainfall is broken.

Over the period 1985–2006, however, the influence of ENSO on the tropical Atlantic is weakened, as displayed in Fig. 15. The correlation between ENSO and tropical Atlantic zonal wind indices is only 0.35, indicating that ENSO can only explain about 12% of the total variance of the regional circulation. Our analysis suggests that decadal changes in the relationship between ENSO and the tropical Atlantic zonal wind might have resulted

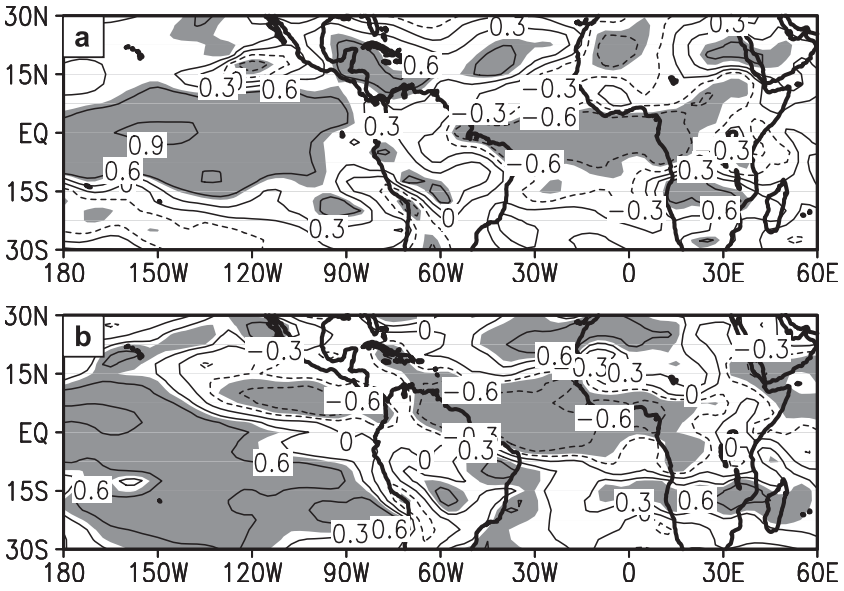

Fig. 13. Correlation maps of (a) March–May 850 hPa zonal wind and (b) June–September 850 hPa zonal wind with the simultaneous ENSO1 index over the period 1970–1984. Shading as in Fig. 3.

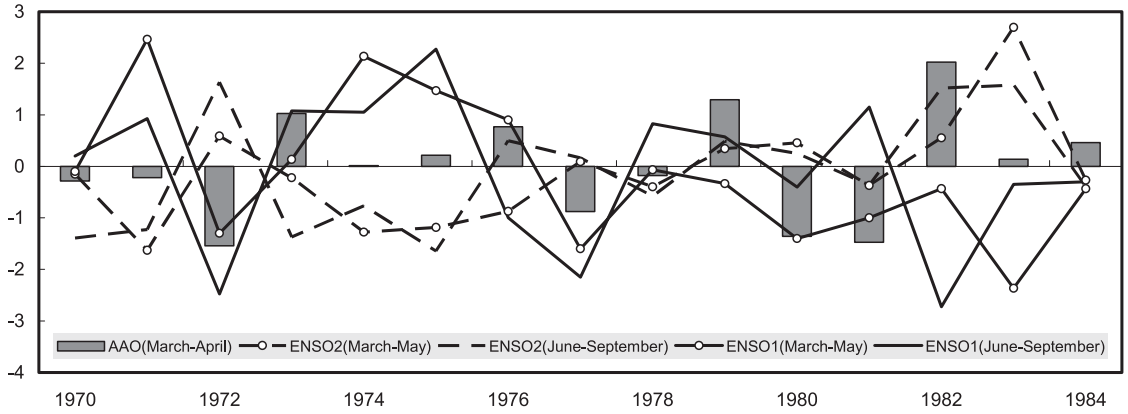

Fig. 14. Normalized time series of the boreal spring AAO, boreal spring ENSO1 and ENSO2, and summer ENSO1 and ENSO2 indices.

from a decadal shift of the ENSO-related circulations. As shown in Fig. 16, in the first period (1970–1985), a significant upward motion related to ENSO is centered over the eastern tropical Pacific (100°W, 0°) and a significant downward motion is centered over the eastern tropical Atlantic (0°, 0°). Such anomalous vertical motions indicate that ENSO variability strongly impacts Walker-like circulation over the eastern tropical Pacific-tropical Atlantic. Thus, there is a significant tropical Atlantic zonal wind anomaly corresponding to an ENSO event, as shown in Fig. 13a. However, in the second period (1985–2006), the ENSO-related vertical motions shift westward, with upward motion over the tropical Pacific west of 120°W and downward motion over the western tropical Atlantic near the coast of South America. Walker-like circulation over the eastern tropical Pacific and tropical Atlantic also shifts westward. Thus, the significant negative zonal wind shifts from the tropical Atlantic in Fig. 13a to tropical South America in Fig. 15a. Over most areas of the tropical Atlantic,

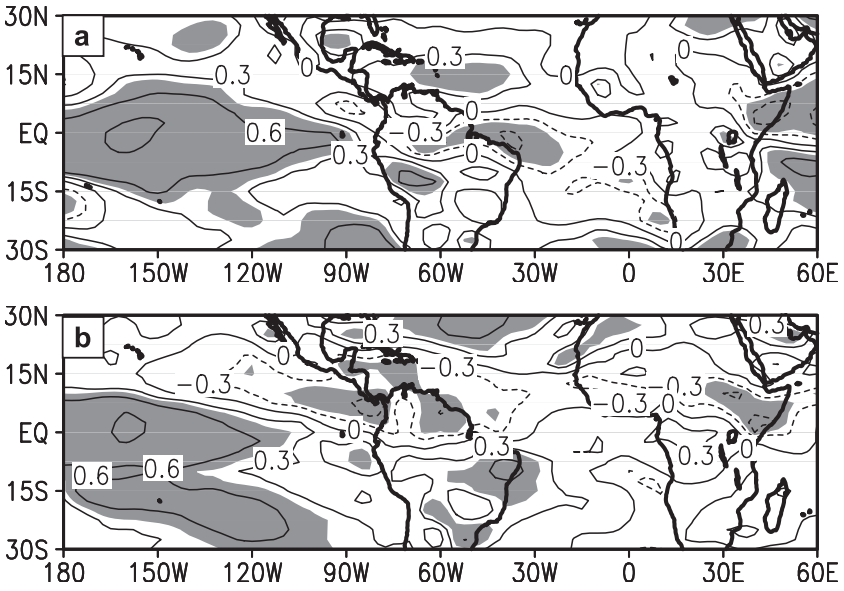

Fig. 15. Correlation maps of (a) March–May 850 hPa zonal wind and (b) June–September 850 hPa zonal wind with the simultaneous ENSO1 index over the period 1985–2006. Shading as in Fig. 3.

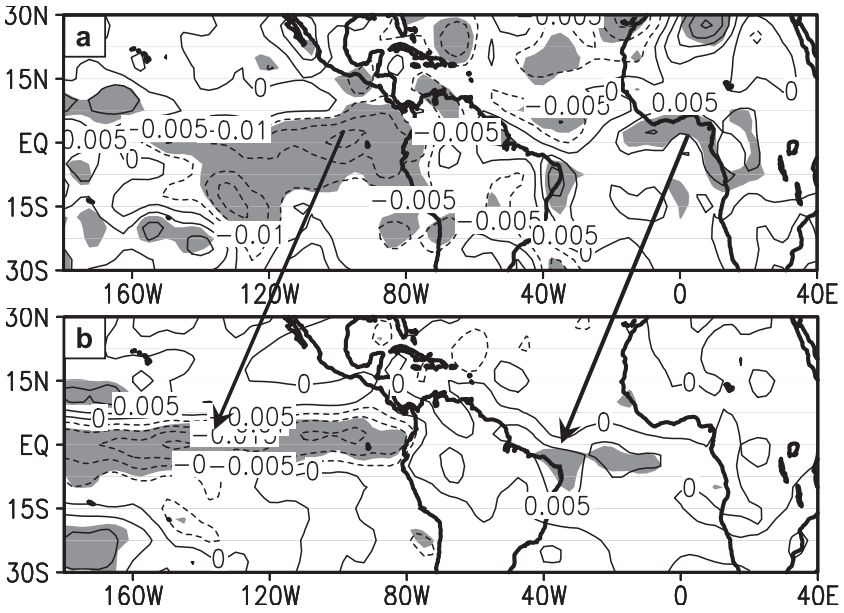

Fig. 16. Regression map of 500 hPa vertical velocity (Pa/s) based on the ENSO1 index in the boreal spring over the periods of (a) 1970–1984 and (b) 1985–2006. Shading as in Fig. 3.

there are no significant large-scale correlations associated with the ENSO events in 1985–2006. Without the strong signal of ENSO in the tropical Atlantic, the influence of the boreal spring AAO could easily reach to the tropical Atlantic, resulting in anomalous tropical South Atlantic SST and MSE and, in turn, in the following anomalous Sahel summer rainfall as discussed previously.

In the observational data, it is difficult to completely separate the independent impact of ENSO and the AAO on tropical Atlantic circulation. In the future, a sensitivity experiment using a climate

model will be needed to investigate the modulation that ENSO provides in the relationship between the boreal spring AAO and Sahel summer rainfall. In addition, our study reveals that decadal shift in ENSO-related circulation occurred around the early 1980s in the boreal spring. The reason for this change is still unknown and needs further detailed exploration.

6. Summary

In this study, we investigate the relationship between the boreal spring AAO and the Sahel summer rainfall. We find that the connection between the two phenomena varies with time. A strong positive correlation between the two exists in 1985–2006, while the correlation is weak between 1970 and 1984. This weak relationship between the two in the earlier period could result from modulation by ENSO events. AAO-related atmospheric circulations back up the correlation analysis. In the strong correlation period, the boreal spring AAO is closely related to the atmospheric circulations associated with the WASM, with a positive AAO corresponding to a strong TEJ and WASM flow. However, in the weak-correlation period, such linkages are broken.

A possible mechanism for the impacts of the boreal spring AAO on the WASM is then discussed, and the physical process is illustrated in the schematic diagram in Fig. 17. In the boreal spring, the AAO influences the tropical South Atlantic SST through a teleconnection pattern from the high-latitude South Pacific to the tropical South Atlantic. The warm (cold) SST can then produce an anomalous MSE over the Guinea-tropical South Atlantic region, consequently changing the MSE meridional gradient between the Sahel and the Guinea-tropical Atlantic region in the boreal spring. The enhanced (suppressed) MSE meridional gradient in the boreal spring can then lead to a strong (weak) WASM (Zheng et al. 1999; Fontaine et al. 2002). This mechanism discussed above is just one possible way to explain the coupling of the boreal spring AAO and WASM. There should be other physical processes linking the two, and further exploration of the subject is needed.

In conclusion, the results shown here indicate that extratropical causes, in addition to tropical forcing, could also play an important role in the variability of the WASM. Thus, a consideration of extratropical causes can help us to better understand and predict the variability of the WASM.

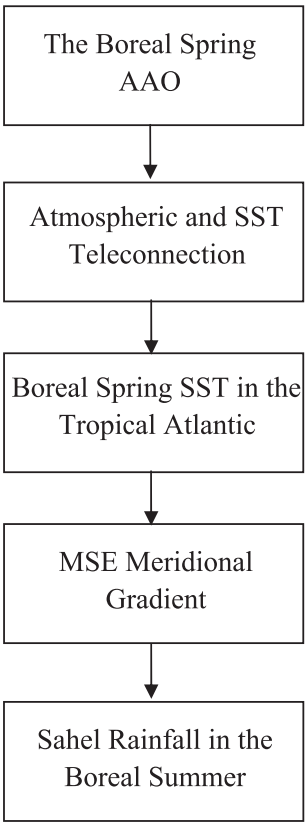

Fig. 17. Schematic diagram showing the coupling process of the boreal spring AAO and the WASM.

Acknowledgments

We would like to thank Prof. Tore Furevik (Bjerknes Centre for Climate Research, Norway), Dr. Kevin Oliver (Department of Earth Sciences, Open University), Dr. Todd P. Mitchell (Joint Institute for the Study of the Atmosphere and Ocean, University of Washington), and two anonymous reviewers for their valuable comments and kind help. This research was jointly supported by the Chinese Academy of Sciences (Grant Nos. KZCX2-YW-217 and KZCX2-YW-Q1-02), the National Basic Research Program of China (Grant No. 2009CB421406), and the National Natural Science Foundation of China (Grant Nos. 40905041 and 40631005).

References

Bader, J., and M. Latif, 2003: The impact of decadal-scale Indian Ocean sea surface temperature anomalies on Sahelian rainfall and the North At-

lantic Oscillation. *Geophys. Res. Lett.*, **30**, 2169, doi: 10.1029/2003GL018426.

Cazes-Boezio, G., A. W. Robertson, and C. R. Mechoso, 2003: Seasonal dependence of ENSO teleconnections over South America and relationships with precipitation in Uruguay. *J. Climate*, **16**, 1159–1176.

Charney, J. G., 1975: Dynamics of deserts and drought in the Sahel. *Quart. J. Roy. Meteor. Soc.*, **101**, 193–202.

Charney, J. G., W. J. Quirk, S. H. Chow, and J. Kornfield, 1977: A comparative study of the effects of albedo change on drought in semi-arid regions. *J. Atmos. Sci.*, **34**, 1366–1385.

Clark, D. B., Y. K. Xue, R. J. Harding, and P. J. Valdes, 2001: Modeling the impact of land surface degradation on the climate of tropical North Africa. *J. Climate*, **14**, 1809–1822.

Deser, C., and M. S. Timlin, 1997: Atmosphere–ocean interaction on weekly timescales in the North Atlantic and Pacific. *J. Climate*, **10**, 393–408.

Eltahir, E. A. B., and C. Gong, 1996: Dynamisc of wet and dry years in West Africa. *J. Climate*, **9**(5), 1030–1042.

Fan, K., and H. J. Wang, 2004: Antarctic oscillation and the dust weather frequency in North China. *Geophys. Res. Lett.*, **31**, L10201, doi:10.1029/2004GL019465.

Ferranti, L., F. Molteni, and T. N. Palmer, 1994: Impact of localized tropical and extratropical SST anomalies in ensembles of seasonal GCM integrations. *Quart. J. Roy. Meteor. Soc.*, **120**, 1613–1645.

Folland, C. K., T. N. Palmer, and D. E. Parker, 1986: Sahel rainfall and worldwide sea temperatures, 1901–85. *Nature*, **320**, 602–607.

Fontaine, B., N. Philippon, S. Trzaska, and P. Roucou, 2002: Spring to summer changes in the West African monsoon through NCEP/NCAR reanalyses (1968–1998). *J. Geophys. Res.*, **107**(D14), 4186, doi:10.1029/2001JD000834.

Frankignoul, C., and R. W. Reynolds, 1983: Testing a dynamical model for midlatitude sea surface temperature anomalies. *J. Phys. Oceanogr.*, **13**, 1131–1145.

Gao, H., F. Xue, and H. J. Wang, 2004: Influence of interannual variability of Antarctic oscillation on Mei-yu along the Yangtze and Huaihe River valley and its importance to prediction. *Chinese Sci. Bull.*, **48**(S2), 61–67.

Giannini, A., R. Saravanan, and P. Chang, 2003: Oceanic forcing of Sahel rainfall on interannual to interdecadal time scales. *Science*, **302**, 1027–1030.

Gong, D. Y., and S. W. Wang, 1999: Definition of Antarctic Oscillation Index. *Geophys. Res. Lett.*, **26**, 459–462.

Grist, J. P., and S. E. Nicholson, 2001: A study of the dynamic factors influencing the rainfall variability in the West African Sahel. *J. Climate*, **14**, 1337–1359.

Hastenrath, S., 1990: Decadal-scale changes of the circulation in the tropical Atlantic sector associated with Sahel drought. *Intl. J. Climatol.*, **10**, 459–472.

Hines, K. M., D. H. Bromwich, and G. J. Marshall, 2000: Artificial surface pressure trends in the NCEP-NCAR reanalysis over the Southern Ocean and Antarctic. *J. Climate*, **13**, 3940–3952.

Huang, J. Y., 2004: Regression analysis. *In Meteorological Statistical Analysis and Forecast Method*, J. Y. Huang (eds.), chapter 2, China Meteorological Press, Beijing, 28–88.

Janicot, S., S. Trzaska, and I. Poccard, 2001: Summer Sahel-ENSO teleconnection and decadal time scale SST variations. *Climate Dyn.*, **18**, 303–320.

Janowiak, J. E., 1988: An investigation of interannual rainfall variability in Africa. *J. Climate*, **1**, 240–255.

Kalnay, E., et al., 1996: The NCEP/NCAR 40-year reanalysis project. *Bull. Amer. Meteor. Soc.*, **77**, 437–471.

Kidson, J. W., 1999: Principal modes of Southern Hemisphere low-frequency variability obtained from NCEP–NCAR reanalyses. *J. Climate*, **12**, 2808–2830.

Kushnir, Y., W. A. Robinson, I. Blade, N. M. J. Hall, S. Peng, and R. Sutton, 2002: Atmospheric GCM response to extratropical SST anomalies: Synthesis and evaluation. *J. Climate*, **15**, 2233–2256.

Lamb, P. J., and R. A. Peppler, 1992: Further case studies of tropical Atlantic surface atmospheric and oceanic patterns associated with sub-Saharan drought. *J. Climate*, **5**, 476–488.

Lebel, T., L. L. Barbe, A. Diedhiou, and A. Amani, 2003: The West African monsoon seasonal cycle. *Exchanges*, **27**, 1–3.

Liebmann, B., G. N. Kiladis, J. A. Marengo, T. Ambrizzi, and J. D. Glick, 1999: Submonthly convective variability over South America and the South Atlantic Convergence Zone. *J. Climate*, **12**, 1877–1891.

Lister, D. H., and J. P. Palutikof, 2001: Seasonal climate forecasting for West Africa: A review, a report produced for the CLIMAG West Africa project: A thematic network supported by the European Commission under the Fifth Framework Programme: Energy, Environment and Sustainable Development Programme Key action 2. Global Change, Climate and Biodiversity ENRICH (European Network for Research on Global Change).

Luksch, U., and H. von Storch, 1992: Modeling the low-frequency sea surface temperature variability in the North Pacific. *J. Climate*, **5**, 893–906.

Matthews, A. J., 2004: Intraseasonal variability over tropical Africa during northern summer. *J. Climate*, **17**, 2427–2440.

Miller, A. J., D. R. Cayan, T. P. Barnett, N. E. Graham, and J. M. Oberhuber, 1994: Interdecadal variability of the Pacific Ocean: Model response to observed heat flux and wind stress anomalies. *Climate Dyn.*, **9**, 287–302.

Moron, V., 2005: Skill of Sahelian rainfall index in two atmospheric general circulation model ensembles forced by prescribed sea surface temperatures. *Exchanges*, **33**, 14 and 19–21.

Nicholson, S. E., 1980: The nature of rainfall fluctuations in subtropical West Africa. *Mon. Wea. Rev.*, **108**, 473–487.

Palmer, T. N., and Z. B. Sun, 1985: A modeling and observational study of the relationship between sea surface temperature in the north-west Atlantic and atmospheric general circulation. *Quart. J. Roy. Meteor. Soc.*, **111**, 947–975.

Plumb, R. A., 1985: On the Three-Dimensional Propagation of Stationary Waves. *J. Atmos. Sci.*, **42**, 217–229.

Rao, P. S., and D. R. Sikka, 2007: Interactive aspects of the Indian and the African summer monsoon systems. *Pure Appl. Geophys.*, **164**, 1699–1716.

Reynolds, R. W., N. A. Rayner, T. M. Smith, D. C. Stokes, and W. Wang, 2002: An improved in situ and satellite SST analysis for climate. *J. Climate*, **15**, 1609–1625.

Rowell, D. P., 2001: Teleconnections between the tropical Pacific and the Sahel. *Quart. J. Roy. Meteor. Soc.*, **127**, 1683–1706.

Rowell, D. P., 2003: The impact of Mediterranean SSTs on the Sahelian rainfall season. *J. Climate*, **16**, 849–862.

Rowell, D. P., C. K. Folland, K. Maskell, and M. N. Ward, 1995: Variability of summer rainfall over tropical North Africa (1906–1992): Observations and modeling. *Quart. J. Roy. Meteor. Soc.*, **121**, 669–704.

Shinoda, M., and R. Kawamura, 1994: Tropical rainbelt, circulation, and sea surface temperatures associated with the Sahelian rainfall trend. *J. Meteor. Soc. Japan*, **72**, 341–357.

Sterl, A., 2004: On the (in)homogeneity of reanalysis products. *J. Climate*, **17**, 3866–3873.

Sud, Y. C., and A. Molod, 1988: A GCM simulation study of the influence of Saharan evapotranspiration and surface-albedo anomalies on July circulation and rainfall. *Mon. Wea. Rev.*, **116**, 2388–2400.

Sun, J. Q., H. J. Wang, and W. Yuan, 2009: A possible mechanism for the co-variability of the boreal spring Antarctic Oscillation and the Yangtze River Valley summer rainfall. *Intl. J. Climatol.*, **29**, 1276–1284, DOI: 10.1002/joc.1773.

Takaya, K., and H. Nakamura, 2001: A Formulation of a Phase-Independent Wave-Activity Flux for Stationary and Migratory Quasigeostrophic Eddies on a Zonally Varying Basic Flow. *J. Atmos. Sci.*, **58**, 608–627.

Thompson, D. W. J., and J. M. Wallace, 2000: Annular modes in the extratropical circulation, Part I: Month-to-month variability. *J. Climate*, **13**, 1000–1016.

Thompson, D. W. J., and S. Solomon, 2002: Interpretation of recent Southern Hemisphere climate change. *Science*, **296**, 895–899.

Uppala, S. M., et al., 2005: The ERA-40 re-analysis. *Quart. J. Roy. Meteor. Soc.*, **131**, 2961–3012.

Vizy, E. K., and K. H. Cook, 2001: Mechanisms by which Gulf of Guinea and eastern North Atlantic sea surface temperature anomalies can influence African rainfall. *J. Climate*, **14**, 795–821.

Wallace, J. M., C. Smith, and Q. Jiang, 1990: Spatial patterns of atmosphere-ocean interaction in the northern winter. *J. Climate*, **3**, 990–998.

Wang, B., R. G. Wu, and K. M. Lau, 2001: Interannual Variability of the Asian Summer Monsoon: Contrasts between the Indian and the Western North Pacific–East Asian Monsoons. *J. Climate*, **14**, 4073–4090.

Wang, G. L., and E. A. B. Eltahir, 2000: Ecosystem dynamics and the Sahel drought. *Geophys. Res. Lett.*, **27**, 795–798.

Wang, H. J., and K. Fan, 2005: Central-north China precipitation as reconstructed from the Qing dynasty: Signal of the Antarctic Atmospheric Oscillation. *Geophys. Res. Lett.*, **32**, L24705, doi:10.1029/2005GL024562.

Xie, P., and P. A. Arkin, 1997: Global precipitation: A 17-year monthly analysis based on gauge observations, satellite estimates and numerical model outputs. *Bull. Amer. Meteor. Soc.*, **78**, 2539–2558.

Xue, F., H. J. Wang, and J. H. He, 2003: Interannual variability of Mascarene high and Australian high and their influences on summer rainfall over East Asia. *Chinese Sci. Bull.*, **48**, 492–497.

Xue, Y. K., and J. Shukla, 1993: The influence of land surface properties on Sahel climate, Part I: Desertification. *J. Climate*, **6**, 2232–2245.

Zeng, N., J. D. Neelin, K. M. Lau, and C. J. Tucker, 1999: Enhancement of interdecadal climate variability in the Sahel by vegetation interaction. *Science*, **286**, 1537–1540.

Zheng, X. Y., E. A. B. Eltahir, and K. A. Emanuel, 1999: A mechanism relating tropical Atlantic spring sea surface temperature and west African rainfall. *Quart. J. Roy. Meteor. Soc.*, **125**, 1129–1163.

Zheng, X. Y., and E. A. B. Eltahir, 1998: The role of vegetation in the dynamics of West African monsoons. *J. Climate*, **11**, 2078–2096.